Systematic low-temperature expansion in the Ginzburg-Landau model

H. C. Kao
Academia Sinica, Institute of Physics, Taipei, Taiwan, Republic of China
and Tamkang University, Department of Physics, Tamsui, Taiwan, Republic of China

B. Rosenstein
Academia Sinica, Institute of Physics, Taipei, Taiwan, Republic of China
and National Center for Theoretical Studies and Electrophysics Department, Naional Chiao Tung University, Hsinchu,
Taiwan, Republic of China

J. C. Lee
National Center for Theoretical Studies and Electrophysics Department, National Chiao Tung University, Hsinchu,
Taiwan, Republic of China
(Received 30 August 1999)

Consistent perturbation theory for thermodynamical quantities in strongly type-II superconductors in a magnetic field at low temperatures is developed. It is complementary to the existing expansion valid at high temperatures. Magnetization and specific heat are calculated to two-loop order and compare well with existing Monte Carlo simulations, other theories, and experiments.

I. INTRODUCTION

Thermal fluctuations play a much larger role in high-T_c superconductors than in the low-temperature ones because the Ginzburg parameter Gi characterizing fluctuations is much larger. In the presence of a magnetic field the importance of fluctuations in high-T_c superconductors is further enhanced. First of all, a strong magnetic field effectively confines long-wavelength fluctuations in a direction perpendicular to the field so that the dimensionality of the fluctuations is reduced by two.[1] Moreover highly anisotropic Bi-Sr-Ca-Cu-O-type layered superconductors are basically two dimensional and one expects a further increase in the importance of fluctuations. Under these circumstances fluctuations influence various physical properties and even lead to new observable qualitative phenomenalike vortex lattice melting into vortex liquid far below the mean-field phase transition line. It is quite straightforward to systematically account for the fluctuation effect on magnetization, specific heat, or conductivity perturbatively above the mean-field transition line using the Ginzburg-Landau (GL) description.[2] However it proved to be extremely difficult to develop a quantitative theory in the most interesting region below this line, even neglecting fluctuation of the magnetic field and within the lowest Landau level (LLL) approximation.

To approach the region below the mean-field transition line $T < T_{mf}(H)$ Thouless[3] proposed a perturbative approach around a homogeneous (liquid) state in which all the ''bubble'' diagrams are resummed. The series provides accurate results at high temperatures, but becomes inapplicable for LLL dimensionless temperature $a_T \sim [T - T_{mf}(H)]/(TH)^{1/2}$ is smaller than 2. See the lines H4–H6 on Fig. 3 for the two-dimensional case, which represent successive approximants (the corresponding three-dimensional plots appear in Ref. 4). Generally, attempts to extend the theory to lower temperature by Padé extrapolation were not successful.[5]

Alternatively, a more direct approach to low-temperature fluctuation physics would be to start from the Abrikosov solution at zero temperature and then take into account perturbatively deviations from this inhomogeneous solution. Experimentally it is reasonable since, for example, specific heat at low temperatures is a smooth function and the fluctuation contribution is quite small. This contrasts sharply with theoretical expectations. A long time ago Eilenberger calculated the spectrum of harmonic excitations of the triangular vortex lattice.[6] Subsequently Maki and Takayama[7] noted that the gapless mode is softer than the usual Goldstone mode expected as a result of spontaneous breaking of translational invariance. The propagator for the phase excitations behaves as $1/(k^2)^2$ in two dimensions (2D). This unexpected additional softness not only enhances the contribution of fluctuations at leading order but also leads to disastrous infrared divergencies apparently at higher orders. As a result, whether the perturbation theory around the vortex state is reliable becomes doubtful. For example the contributions to free energy depicted in Figs. 2(a) and 2(d) are, respectively, L^4 and $\ln^2(L)$ divergent [L being an infrared (IR) cutoff] in 3D and the divergencies get worse at higher orders. In 2D, the situation is aggravated: the diagrams diverge as L^8 and L^4. Also qualitatively the lower critical dimensionality for melting of the Abrikosov lattice is $D_c = 3$ and consequently an infinite range vortex lattice in clean materials exists only at $T = 0$. One, therefore, tends to think that nonperturbative effects are so important that such a perturbation theory should be abandoned.[8] However, a closer look at the diagrams like Fig. 2(a) (see details below) reveals that in fact one encounters actually only milder divergencies in both 2D and 3D. This makes the divergencies similar to the so-called spurious divergencies in the theory of critical phenomena with broken continuous symmetry. In such a case one can prove[9] that

they exactly cancel at each order provided we are calculating a symmetric quantity.

In this paper we show that all the IR divergencies in free energy or other quantities invariant under translations cancel to the two-loop order. The three-dimensional case was briefly reported in Ref. 4, here we present in detail the more complicated two-dimensional case. We calculate magnetization and specific heat to this order and compare the results with existing high-temperature expansion, Monte Carlo (MC) simulation[10] of the same system, and experiments. Qualitatively the physics of a fluctuating three-dimensional GL model in a magnetic field turns out to be similar to that of two-dimensional spin systems (or scalar fields) possessing a continuous symmetry. In particular, although within perturbation theory the ordered phase (solid) exists only at $T=0$, in the thermodynamic limit, at low temperatures, solid with powerwise decay of the translational order or liquid (exponential decay) differs very little from the solid in most aspects. Therefore, one can effectively use properly modified perturbation theory to study quantitatively various properties of the vortex liquid phase. Similarly physics of the two-dimensional GL model is analogous to that of the one-dimensional scalar theory with, say $O(2)$ symmetry. This is equivalent to the anharmonic oscillator in quantum mechanics or the XY spin chain in statistical physics.

This paper is organized as follows. In Sec. II the model is introduced and the Feynman rules for the loop (low temperature) expansion within the LLL approximation are set up. The free energy to two loops is calculated using diagrammatic expansion in Sec. III. It is shown how all the infrared divergencies cancel exactly at least up to two-loop order. In Sec. IV we compare the present expansion with the high-temperature series, theory of Tesanovic et al.,[11] available MC simulations, and experiments. In Sec. V we discuss qualitatively nonperturbative effects using the analogy with magnetic systems mentioned above. We exemplify this by calculating perturbatively the ground-state energy of the $O(2)$ invariant one-dimensional chain (equivalent to the quantum-mechanical anharmonic oscillator) that exhibits similar IR divergencies. We argue that although the infinite range translational order is not present in this system, locally the system looks like a lattice and the perturbative results are valid up to exponential corrections. Finally, we briefly summarize the results and discuss the melting transition observed in experiments and some MC simulations, contributions of higher LL, and fluctuations of the magnetic field in Sec. VII.

II. MODEL, MEAN-FIELD SOLUTION, AND THE PERTURBATION THEORY

A. Two-dimensional Ginzburg-Landau model

Our starting point is the GL free energy

$$F = L_z \int d^2x \frac{\hbar^2}{2m} \left| \left(\nabla - \frac{ie^*}{\hbar c} \mathbf{A} \right) \psi \right|^2 + a|\psi|^2 + \frac{b'}{2}|\psi|^4. \quad (1)$$

Here $\mathbf{A} = (-By, 0)$ describes a nonfluctuating constant magnetic field in Landau gauge and its energy density is dropped for convenience. In strongly type-II superconductors ($\kappa \sim 100$), far from H_{c1} (this is the range of interest in this paper) the magnetic field is homogeneous to a high degree

due to superposition from many vortices. For simplicity we assume $a = -\alpha' T_c(1-t)$, $t \equiv T/T_c$ although this dependence can be easily modified to better describe the experimental coherence length.

Throughout most of the paper the following units will be used. Unit of length is $\xi = \sqrt{\hbar^2/(2m_{ab}\alpha'T_c)}$ and unit of magnetic field is H_{c2}, so that the dimensionless magnetic field is $b \equiv B/H_{c2}$. The dimensionless free energy in these units is [the order parameter field is rescaled as $\psi^2 \rightarrow (2\alpha'T_c/b')\psi^2$]

$$\frac{F}{T} = \frac{1}{\omega} \int d^2x \left[\frac{1}{2}|\mathbf{D}\psi|^2 - \frac{1-t}{2}|\psi|^2 + \frac{1}{2}|\psi|^4 \right], \quad (2)$$

with $\mathbf{D} = \nabla - (ie^*/\hbar c)\mathbf{A}$. The dimensionless coefficient is

$$\omega = \sqrt{2Gi}\,\pi^2 t, \quad (3)$$

where the Ginzburg number is defined by $Gi \equiv \frac{1}{2}(32\pi e^2\kappa^2\xi^2 T_c/L_z c^2 h^2)^2$. The coefficient ω determines the strength of fluctuations, but is irrelevant as far as mean-field solutions are concerned.

B. Mean-field solution near H_{c2}

Defining the operator $\mathcal{H} \equiv \frac{1}{2}(-\mathbf{D}^2 - b)$, the free energy becomes

$$\frac{F}{T} = \frac{1}{\omega} \int d^2x \left[\psi^* \mathcal{H}\psi - a_h|\psi|^2 + \frac{1}{2}|\psi|^4 \right]. \quad (4)$$

Here,

$$a_h \equiv \frac{1-t-b}{2} \quad (5)$$

is the second expansion parameter. If a_h is sufficiently small, GL equations can be solved perturbatively (see Refs. 12 and 13 for details):

$$\Phi = \sqrt{\frac{a_h}{\beta_A}} \varphi(\mathbf{x}) + O(a_h^{3/2}), \quad (6)$$

where $\beta_A = 1.16$ and

$$\varphi(\mathbf{x}) = \left(\frac{2\pi b}{\sqrt{\pi}a_\triangle} \right)^{1/2} \sum_{l=-\infty}^{\infty} \exp\left\{ i\left[\frac{\pi l(l-1)}{2} + \frac{2\pi}{a_\triangle}l\sqrt{b}x \right] \right.$$
$$\left. -\frac{1}{2}\left(\sqrt{b}y - \frac{2\pi}{a_\triangle}l \right)^2 \right\}. \quad (7)$$

The lattice spacing is given by $a_\triangle/\sqrt{b}$, with $a_\triangle = \sqrt{4\pi/\sqrt{3}}$ and $1/\sqrt{b}$ the magnetic length in our units. It is normalized to the unit average $\langle|\varphi|^2\rangle = 1$.

C. Fluctuations and Feynman rules

Within the LLL approximation, which will be used here, the above solution becomes exact so higher orders in a_h do not appear and ψ can be expanded in a basis of quasimomentum $\mathbf{k}$ eigenfunctions
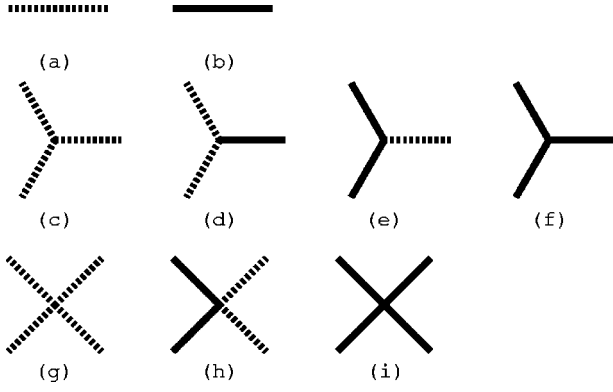
FIG. 1. All the relevant propagators and vertices in the theory. Here, dashed and solid lines represent the A and O fields, respectively.

$$\varphi_{\mathbf{k}} = \left(\frac{2\pi b}{\sqrt{\pi} a_{\triangle}}\right)^{1/2} \sum_{l=-\infty}^{\infty} \exp\left\{i\left[\frac{\pi l(l-1)}{2} + \frac{2\pi}{a_{\triangle}}l\left(\sqrt{b}x + \frac{k_y}{\sqrt{b}}\right)\right.\right.$$

$$\left.\left. + xk_x\right] - \frac{1}{2}\left(\sqrt{b}y - \frac{k_x}{\sqrt{b}} - \frac{2\pi}{a_{\triangle}}l\right)^2\right\},$$

around the mean field solution

$$\psi(x) = v\,\varphi(x) + \int_{BZ}\frac{d^2k}{(2\pi)^2}\varphi_{\mathbf{k}}(x)c_{\mathbf{k}}(O_{\mathbf{k}} + iA_{\mathbf{k}}). \quad (8)$$

The shift v of the fluctuating field will be generally different from its mean-field value. The integration is over a Brillouin zone of the hexagonal lattice that has an area 2π. $O_{\mathbf{k}}$ and $A_{\mathbf{k}}$ are ''real'' fields satisfying $O_{\mathbf{k}}^* = O_{-\mathbf{k}}$, $A_{\mathbf{k}}^* = A_{-\mathbf{k}}$. They are somewhat analogous to the acoustic and optical phonons in usual solids with some peculiarities due to a strong magnetic field.[5] For example, the A mode corresponds to shear of the two-dimensional lattice. After we substitute Eq. (8) into the free energy, the quadratic terms in the fields define propagators, while the cubic and quartic terms give rise to interactions. The phase factors $c_{\mathbf{k}} \equiv \sqrt{\gamma_{\mathbf{k}}/2|\gamma_{\mathbf{k}}|}$ with $\gamma_{\mathbf{k}} \equiv \int_x \varphi_{\mathbf{k}}^*(x)\varphi_{-\mathbf{k}}^*(x)\varphi(x)\varphi(x)$ are introduced in order to diagonalize the resulting quadratic part of the free energy

$$F_{quad} = \frac{1}{2}\int_{BZ}\frac{d^2k}{(2\pi)^2}[P_O^{-1}(\mathbf{k})O_{\mathbf{k}}^*O_{\mathbf{k}} + P_A^{-1}(\mathbf{k})A_{\mathbf{k}}^*A_{\mathbf{k}}]. \quad (9)$$

Here, $P_{O,A}(\mathbf{k})$ are the propagators entering the Feynman diagrams in Figs. 1(a) and 1(b) and are given by

$$P_{O,A}(\mathbf{k}) = M_{O,A}^{-2}(\mathbf{k}), \quad M_{O,A}^{-2}(\mathbf{k}) = -a_h + v^2(2\beta_{\mathbf{k}} \pm |\gamma_{\mathbf{k}}|), \quad (10)$$

with $\beta_{\mathbf{k}} \equiv \int_x \varphi_{\mathbf{k}}^*(x)\varphi^*(x)\varphi_{\mathbf{k}}(x)\varphi(x)$.

For convenience, let us introduce the function $\lambda(\mathbf{k}_1, \mathbf{k}_2)$:

$$\lambda(\mathbf{k}_1, \mathbf{k}_2) = \left(\frac{\sqrt{3}}{2}\right)^{1/2}\exp\left\{-\frac{(k_1^x)^2 + (k_2^x)^2}{2}\right\} \quad (11)$$

$$\sum_{l,m}(-)^{lm}\exp\left\{i\frac{2\pi}{a_{\triangle}}[lk_1^y + mk_2^y]\right.$$

$$\left. - \frac{1}{2}\left[\left(k_2^x + \frac{2\pi}{a_{\triangle}}l\right)^2 + \left(k_1^x + \frac{2\pi}{a_{\triangle}}m\right)^2\right]\right\}. \quad (12)$$

Now, the various functions encountered so far, as well as all the three- and four-leg vertices, can be expressed in terms of it: for example, $\gamma_{\mathbf{k}} = \lambda(-\mathbf{k}, \mathbf{k})$, $\beta_{\mathbf{k}} = \lambda(0, \mathbf{k})$. The vertices are depicted in Figs. 1(c)–1(i) with the following expressions. Three leg vertices:

(c) $\quad A_{\mathbf{k}_1}A_{\mathbf{k}_2}A_{-\mathbf{k}_1-\mathbf{k}_2} = -2v\,\mathrm{Im}[\lambda(\mathbf{k}_2, \mathbf{k}_1$

$$+ \mathbf{k}_2)c_{\mathbf{k}_1}^*c_{\mathbf{k}_2}c_{\mathbf{k}_1+\mathbf{k}_2}], \quad (13)$$

(d) $\quad A_{\mathbf{k}_1}A_{\mathbf{k}_2}O_{-\mathbf{k}_1-\mathbf{k}_2} = 2v\,\mathrm{Re}[-\lambda(\mathbf{k}_1, -\mathbf{k}_2)c_{\mathbf{k}_1}c_{\mathbf{k}_2}c_{\mathbf{k}_1+\mathbf{k}_2}^*$

$$+ 2\lambda(-\mathbf{k}_1 - \mathbf{k}_2,$$

$$- \mathbf{k}_2)c_{\mathbf{k}_1}^*c_{\mathbf{k}_2}c_{\mathbf{k}_1+\mathbf{k}_2}], \quad (14)$$

(e) $\quad O_{\mathbf{k}_1}O_{\mathbf{k}_2}A_{-\mathbf{k}_1-\mathbf{k}_2} = -2v\,\mathrm{Im}[-\lambda(\mathbf{k}_1, 2\mathbf{k}_1$

$$+ \mathbf{k}_2)c_{\mathbf{k}_1}^*c_{\mathbf{k}_2}c_{\mathbf{k}_1+\mathbf{k}_2} + 2\lambda(\mathbf{k}_1,$$

$$- \mathbf{k}_2)c_{\mathbf{k}_1}c_{\mathbf{k}_2}c_{\mathbf{k}_1+\mathbf{k}_2}^*], \quad (15)$$

(f) $\quad O_{\mathbf{k}_1}O_{\mathbf{k}_2}O_{-\mathbf{k}_1-\mathbf{k}_2} = 2v\,\mathrm{Re}[\lambda(\mathbf{k}_2, \mathbf{k}_1+\mathbf{k}_2)c_{\mathbf{k}_1}^*c_{\mathbf{k}_2}c_{\mathbf{k}_1+\mathbf{k}_2}]. \quad (16)$

Four leg vertices:

(g) $\quad A_{\mathbf{k}_1}A_{\mathbf{k}_2}A_{\mathbf{k}_3}A_{-\mathbf{k}_1-\mathbf{k}_2-\mathbf{k}_3}$

$$= \frac{1}{2}\mathrm{Re}[\lambda(\mathbf{k}_1+\mathbf{k}_3, \mathbf{k}_2+\mathbf{k}_3)c_{\mathbf{k}_1}^*c_{\mathbf{k}_2}^*c_{\mathbf{k}_3}c_{\mathbf{k}_1+\mathbf{k}_2+\mathbf{k}_3}], \quad (17)$$

(h) $\quad A_{\mathbf{k}_1}A_{\mathbf{k}_2}O_{\mathbf{k}_3}O_{-\mathbf{k}_1-\mathbf{k}_2-\mathbf{k}_3}$

$$= \mathrm{Re}[-\lambda(\mathbf{k}_1+\mathbf{k}_3, \mathbf{k}_2+\mathbf{k}_3)c_{\mathbf{k}_1}^*c_{\mathbf{k}_2}^*c_{\mathbf{k}_3}c_{\mathbf{k}_1+\mathbf{k}_2+\mathbf{k}_3} \quad (18)$$

$$+ 2\lambda(\mathbf{k}_1+\mathbf{k}_3, \mathbf{k}_1+\mathbf{k}_2)c_{\mathbf{k}_1}c_{\mathbf{k}_2}^*c_{\mathbf{k}_3}^*c_{\mathbf{k}_1+\mathbf{k}_2+\mathbf{k}_3}], \quad (19)$$

(i) $\quad O_{\mathbf{k}_1}O_{\mathbf{k}_2}O_{\mathbf{k}_3}O_{-\mathbf{k}_1-\mathbf{k}_2-\mathbf{k}_3} = \frac{1}{2}\mathrm{Re}[\lambda(\mathbf{k}_1+\mathbf{k}_3, \mathbf{k}_2$

$$+ \mathbf{k}_3)c_{\mathbf{k}_1}^*c_{\mathbf{k}_2}^*c_{\mathbf{k}_3}c_{\mathbf{k}_1+\mathbf{k}_2+\mathbf{k}_3}]. \quad (20)$$

III. CANCELLATION OF INFRARED DIVERGENCIES IN LOOP EXPANSION

A. One loop free energy, ''field shift,'' and destruction of the infinite range translation order by fluctuations

If the fluctuations were absent the expectation value $v_0^2 = a_h/\beta_A$ would minimize $G_0 = -a_h v^2 + \frac{1}{2}\beta_A v^4$. The one-loop contribution to the free energy is
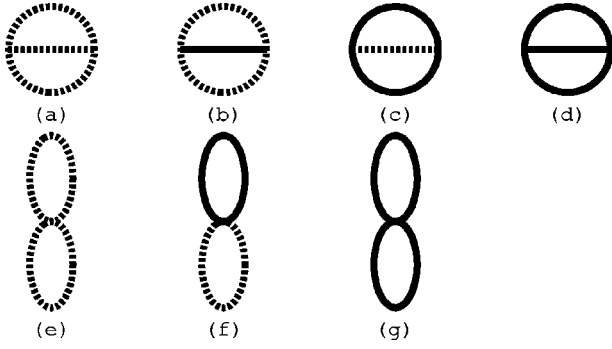
FIG. 2. Setting-sun and double-bubble diagrams that contribute to the free energy at the two-loop level.

$$G_1 = \frac{1}{2} \frac{1}{(2\pi)^2} \int_{\mathbf{k}} \{\ln[M_O^2(\mathbf{k})] + \ln[M_A^2(\mathbf{k})]\}. \quad (21)$$

To this order the free energy that is a symmetric quantity is convergent. However the expectation value of the field that is not a symmetric quantity is divergent. Minimizing $G_0 + G_1$ with respect to v would lead to the following correction to the vacuum expectation value:

$$v_1^2 = \frac{1}{2} \frac{1}{(2\pi)^2} \int_{\mathbf{k}} \left\{ \frac{[2\beta_{\mathbf{k}} + |\gamma_{\mathbf{k}}|]}{M_O^2(\mathbf{k})} + \frac{[2\beta_{\mathbf{k}} - |\gamma_{\mathbf{k}}|]}{M_A^2(\mathbf{k})} \right\}. \quad (22)$$

Due to additional softness of the A mode, the above integral diverges in the infrared region. This means that the fluctuations destroy the inhomogeneous ground state, namely, the state with lowest energy is a homogeneous liquid in accord with the fact that the lower critical dimension for the present model is $D = 3$.[4] It, however, does not necessarily mean that perturbation theory starting from an ordered ground state is inapplicable. The way to proceed in such situations has been found while considering simpler models like the one-dimensional φ^4 model $F = \frac{1}{2}(\nabla \varphi_a)^2 + V(\varphi_a^2)$, $a = 1,2$ discussed in detail in Sec. V (see also Ref. 14).

B. Two-loop contributions to the free energy

To the two-loop order one gets several classes of diagrams (see Fig. 2): the setting sun (AAA, AAO, AOO, OOO), double bubble (AA, AO, OO), and the ''correction term'' (AA, AA, OO), which arises due to a correction in the value of v from Eq. (22) . All of them can be expressed explicitly in terms of the function $\lambda(\mathbf{k}_1, \mathbf{k}_2)$ and $d_{\mathbf{k}} \equiv 2c_{\mathbf{k}}^2$.

1. Setting-sun diagrams

The setting-sun diagrams are shown in Figs. 2(a)–2(d). The AAA diagram is naively the most divergent one among them.

$$(a) \quad AAA = \frac{-v^2}{8(2\pi)^2} \int_{\mathbf{p}} \int_{\mathbf{q}} \frac{I_{ssAAA}(\mathbf{p},\mathbf{q})}{M_A^2(\mathbf{p})M_A^2(\mathbf{q})M_A^2(\mathbf{p+q})}; \quad (23)$$

$$I_{ssAAA}(\mathbf{p},\mathbf{q}) \equiv |\lambda(\mathbf{p},-\mathbf{q})|^2 - \lambda^2(\mathbf{p},-\mathbf{q})d_{\mathbf{p}}d_{\mathbf{q}}d_{\mathbf{p+q}}^* + 2\lambda(\mathbf{p},$$
$$-\mathbf{q})\lambda(\mathbf{p},-\mathbf{p}-\mathbf{q})d_{\mathbf{q}}d_{\mathbf{p+q}}^* - 2\lambda(\mathbf{p},-\mathbf{q})\lambda^*(\mathbf{p},$$
$$-\mathbf{p}-\mathbf{q})d_{\mathbf{p}} + \text{c.c.}$$

$$(b) \quad AAO = \frac{-v^2}{8(2\pi)^2} \int_{\mathbf{q}} \int_{\mathbf{p}} \frac{I_{ssAAO}(\mathbf{p},\mathbf{q})}{M_A^2(\mathbf{p})M_A^2(\mathbf{q})M_O^2(\mathbf{p+q})}; \quad (24)$$

$$I_{ssAAO}(\mathbf{p},\mathbf{q}) \equiv |\lambda(\mathbf{p},-\mathbf{q})|^2 + \lambda(\mathbf{p},-\mathbf{q})^2 d_{\mathbf{p}}d_{\mathbf{q}}d_{\mathbf{p+q}}^* + 2|\lambda(\mathbf{p}$$
$$+\mathbf{q},\mathbf{p})|^2 + 2\lambda(\mathbf{p}+\mathbf{q},\mathbf{p})^2 d_{\mathbf{p}}d_{\mathbf{q}}d_{\mathbf{p+q}} - 4\lambda(\mathbf{p},$$
$$-\mathbf{q})\lambda(\mathbf{p}+\mathbf{q},\mathbf{p})d_{\mathbf{p}} - 4\lambda(\mathbf{p},-\mathbf{q})\lambda^*(\mathbf{p}$$
$$+\mathbf{q},\mathbf{p})d_{\mathbf{q}}d_{\mathbf{p+q}}^* + 4\lambda(\mathbf{p}+\mathbf{q},\mathbf{p})\lambda^*(\mathbf{p}+\mathbf{q},\mathbf{q})d_{\mathbf{p}}d_{\mathbf{q}}$$
$$+ 4\lambda(\mathbf{p}+\mathbf{q},\mathbf{p})\lambda(\mathbf{p}+\mathbf{q},\mathbf{q})d_{\mathbf{p+q}} + \text{c.c.}$$

$$(c) \quad AOO = \frac{-v^2}{8(2\pi)^2} \int_{\mathbf{q}} \int_{\mathbf{p}} \frac{I_{ssAOO}(\mathbf{q},\mathbf{p})}{M_O^2(\mathbf{p})M_O^2(\mathbf{q})M_A^2(\mathbf{p+q})}; \quad (25)$$

$$I_{ssAOO}(\mathbf{p},\mathbf{q}) \equiv |\lambda(\mathbf{p},-\mathbf{q})|^2 - \lambda(\mathbf{p},-\mathbf{q})^2 d_{\mathbf{p}}d_{\mathbf{q}}d_{\mathbf{p+q}}^* + 2|\lambda(\mathbf{p}$$
$$+\mathbf{q},\mathbf{p})|^2 - 2\lambda(\mathbf{p}+\mathbf{q},\mathbf{p})^2 d_{\mathbf{p}}d_{\mathbf{q}}d_{\mathbf{p+q}} + 4\lambda(\mathbf{p},$$
$$-\mathbf{q})\lambda(\mathbf{p}+\mathbf{q},\mathbf{p})d_{\mathbf{p}} - 4\lambda(\mathbf{p},-\mathbf{q})\lambda^*(\mathbf{p}$$
$$+\mathbf{q},\mathbf{p})d_{\mathbf{q}}d_{\mathbf{p+q}}^* + 4\lambda(\mathbf{p}+\mathbf{q},\mathbf{p})\lambda^*(\mathbf{p}$$
$$+\mathbf{q},\mathbf{q})d_{\mathbf{p}}d_{\mathbf{q}} - 4\lambda(\mathbf{p}+\mathbf{q},\mathbf{p})\lambda(\mathbf{p}+\mathbf{q},\mathbf{q})d_{\mathbf{p+q}}$$
$$+ \text{c.c.}$$

$$(d) \quad OOO = \frac{-v^2}{8(2\pi)^2} \int_{\mathbf{q}} \int_{\mathbf{p}} \frac{I_{ssOOO}(\mathbf{p},\mathbf{q})}{M_O^2(\mathbf{p})M_O^2(\mathbf{q})M_O^2(\mathbf{p+q})}; \quad (26)$$

$$I_{ssOOO}(\mathbf{p},\mathbf{q}) \equiv |\lambda(\mathbf{p},-\mathbf{q})|^2 + \lambda(\mathbf{p},-\mathbf{q})^2 d_{\mathbf{p}}d_{\mathbf{q}}d_{\mathbf{p+q}}^* + 2\lambda(\mathbf{p},$$
$$-\mathbf{q})\lambda(\mathbf{p},-\mathbf{p}-\mathbf{q})d_{\mathbf{q}}d_{\mathbf{p+q}}^* + 2\lambda(\mathbf{p},$$
$$-\mathbf{q})\lambda^*(\mathbf{p},-\mathbf{p}-\mathbf{q})d_{\mathbf{p}} + \text{c.c.}$$

2. Double-bubble diagrams

The bubble diagrams are shown in Figs. 2(e)–2(g).

$$(e) \quad AA = \frac{1}{8(2\pi)^2} \int_{\mathbf{p}} \int_{\mathbf{q}} \frac{I_{bbAA}(\mathbf{p},\mathbf{q})}{M_A^2(\mathbf{p})M_A^2(\mathbf{q})}; \quad (27)$$

$$I_{bbAA}(\mathbf{p},\mathbf{q}) \equiv \lambda(-\mathbf{p}+\mathbf{q},\mathbf{p}+\mathbf{q})d_{\mathbf{p}}d_{\mathbf{q}} + 2\beta_{\mathbf{p}-\mathbf{q}} + \text{c.c.}$$

$$(f) \quad AO = \frac{2}{8(2\pi)^2} \int_{\mathbf{q}} \int_{\mathbf{p}} \frac{I_{bbAO}(\mathbf{p},\mathbf{q})}{M_A^2(\mathbf{p})M_O^2(\mathbf{q})}; \quad (28)$$

$$I_{bbAO}(\mathbf{p},\mathbf{q}) \equiv -\lambda(-\mathbf{p}+\mathbf{q},\mathbf{p}+\mathbf{q})d_{\mathbf{p}}d_{\mathbf{q}} + 2\beta_{\mathbf{p}-\mathbf{q}} + \text{c.c.}$$

$$(g) \quad OO = \frac{1}{8(2\pi)^2} \int_{\mathbf{q}} \int_{\mathbf{p}} \frac{I_{bbOO}(\mathbf{p},\mathbf{q})}{M_O^2(\mathbf{p})M_O^2(\mathbf{q})}; \quad (29)$$

$$I_{bbOO}(\mathbf{p},\mathbf{q}) \equiv \lambda(-\mathbf{p}+\mathbf{q},\mathbf{p}+\mathbf{q})d_{\mathbf{p}}d_{\mathbf{q}} + 2\beta_{\mathbf{p}-\mathbf{q}} + \text{c.c.}$$

3. Shift-correction terms

The shift-correction terms are given by

$$AA = \frac{-1}{8(2\pi)^2} \int_{\mathbf{p}} \int_{\mathbf{q}} \frac{I_{crAA}(\mathbf{p},\mathbf{q})}{M_A^2(\mathbf{p})M_A^2(\mathbf{q})}; \qquad (30)$$

$$I_{crAA}(\mathbf{p},\mathbf{q}) \equiv (2\beta_{\mathbf{p}} - |\gamma_{\mathbf{p}}|)(2\beta_{\mathbf{q}} - |\gamma_{\mathbf{q}}|).$$

$$AO = \frac{-2}{8(2\pi)^2} \int_{\mathbf{q}} \int_{\mathbf{p}} \frac{I_{ccAO}(\mathbf{p},\mathbf{q})}{M_A^2(\mathbf{p})M_O^2(\mathbf{q})}; \qquad (31)$$

$$I_{crAO}(\mathbf{p},\mathbf{q}) \equiv (2\beta_{\mathbf{p}} - |\gamma_{\mathbf{p}}|)(2\beta_{\mathbf{q}} + |\gamma_{\mathbf{q}}|).$$

$$OO = \frac{-1}{8(2\pi)^2} \int_{\mathbf{q}} \int_{\mathbf{p}} \frac{I_{crOO}(\mathbf{p},\mathbf{q})}{M_O^2(\mathbf{p})M_O^2(\mathbf{q})}; \qquad (32)$$

$$I_{crOO}(\mathbf{p},\mathbf{q}) \equiv (2\beta_{\mathbf{p}} + |\gamma_{\mathbf{p}}|)(2\beta_{\mathbf{q}} + |\gamma_{\mathbf{q}}|).$$

C. Cancellations of IR divergence within diagrams

To analyze the IR divergence, one needs to expand the propagators and vertices around small quasimomentum. Using the explicit expansion for $\lambda(\mathbf{k}_1,\mathbf{k}_2)$ given in the Appendix, one can in turn find those for $\gamma_{\mathbf{k}}$, $\beta_{\mathbf{k}}$, and $d_{\mathbf{k}}$. It turns out that the constant and k^2 terms in $M_A^2(\mathbf{k})$ vanish, so that the (only) leading quartic term is $-\frac{1}{4}a_h(\beta_{22}/\beta_A)|\mathbf{k}|^4$ and $M_O^2(\mathbf{k}) = a_h[2 - |\mathbf{k}|^2 + (\frac{1}{4} - \frac{1}{4}\beta_{22}/\beta_A)|\mathbf{k}|^4]$. Here,

$$\beta_{st} \equiv \left(\frac{\sqrt{3}}{2}\right)^{1/2} \left(\frac{2\pi}{a_\triangle}\right)^{s+t} \sum_{l,m} (-)^{lm} l^s m^t$$

$$\times \exp\left[-\frac{(2\pi)^2}{2a_\triangle^2}(l^2 + m^2)\right]. \qquad (33)$$

As a result, the leading divergence $\sim \int_{\mathbf{p}} \int_{\mathbf{q}} I_{ssAAA}(\mathbf{p},\mathbf{q})/|\mathbf{p}|^4 |\mathbf{q}|^4 |\mathbf{q}+\mathbf{p}|^4$ is determined by the asymptotics of $I_{ssAAA}(\mathbf{p},\mathbf{q})$ as both $\mathbf{p}$ and $\mathbf{q}$ approach zero. If $I_{ssAAA} \sim 1$, it would diverge as L^8. However the vertex is "supersoft" at small quasimomenta so that the divergence is milder than expected. For example, the $A_{\mathbf{k}_1}A_{\mathbf{k}_2}A_{-\mathbf{k}_1-\mathbf{k}_2}$ vertex expansion at small momenta starts with $(k_1^x k_2^y + k_1^y k_2^x)$. Therefore, the leading divergence is "just" L^4. Expanding $I_{ssAAA}(\mathbf{p},\mathbf{q})$ around $\mathbf{p}=\mathbf{q}=0$, we see that actually $I_{ssAAA}(\mathbf{p},\mathbf{q}) \propto O(p^8)$:

$$I_{ssAAA}(\mathbf{p},\mathbf{q}) = \left(\frac{1}{4}\beta_{00} - \beta_{22}\right)^2 [p^2 q^2 - (pq)^2](p^2 - q^2)(p^2 + q^2 + 4pq).$$

As a matter of fact, it even becomes $O(p^{10})$ after we symmetrize it with respect to $\mathbf{p} \leftrightarrow \mathbf{q}$, and the diagram is actually finite. Similarly an apparent logarithmic divergence in setting sun AOO is nonexistent.

D. Cancellation between different diagrams

After the *a priori* most divergent diagram turned out to be convergent we look for milder IR divergencies in other diagrams. The remaining most divergent terms appear in contributions ss_{AAO}, bb_{AA}, and cr_{AA}, and come from the quasi-momentum independent terms in the numerator of the integrands:

$$I_{ssAAO} = 4\beta_{00}^2, \quad I_{bbAA} = 3\beta_{00}, \quad I_{crAA} = \beta_{00},$$

respectively. Although they are L^4 divergent by themselves, their sum with appropriate coefficients $-(2\beta_{00})^{-1}, 1$, and -1 cancels. The order L^2 divergencies come from the following integrands:

$$I_{ssAAO} = -4\beta_{00}^2(p^2 + q^2 + 2pq),$$

$$I_{bbAA} = \beta_{00}(-p^2 - q^2 + pq).$$

Expanding $M_O^2(\mathbf{p}+\mathbf{q})$ in the denominator to the second order in quasimomenta, we see they cancel each other after symmetrization with respect to $\mathbf{p} \leftrightarrow \mathbf{q}$ and $\mathbf{p} \leftrightarrow -\mathbf{p}$. Finally, there are five $\ln(L)$ divergent terms:

$$I_{ssAAO} = \frac{1}{4}\beta_{00}^2[9p^4 + 7q^4 + (pq)(36p^2 + 28q^2) + 12p^2 q^2$$
$$+ 36(pq)^2] - 2\beta_{00}\beta_{22}[2(pq)(p^2 + q^2) - p^2 q^2$$
$$+ 6(pq)^2],$$

$$I_{bbAA} = \frac{1}{4}\beta_{00}[p^4 + q^4 - (2pq)(p^2 + q^2) + 6(pq)^2]$$
$$- \frac{1}{4}\beta_{22}[p^4 + q^4 - 4(pq)(p^2 + q^2) - 6p^2 q^2$$
$$+ 20(pq)^2],$$

$$I_{bbAO} = \beta_{00},$$

$$I_{crAA} = -\frac{1}{4}\beta_{22}[p^4 + q^4],$$

$$I_{crAO} = 3\beta_{00}.$$

By symmetrizing the sum of all five terms, we see the final result is indeed free of IR divergence.

IV. COMPARISON OF RESULTS WITH OTHER THEORIES AND EXPERIMENTS

A. Comparison with high-temperature expansion

The same theory has been studied by various analytical and numerical methods. To compare our results with those obtained using other methods, let us restore the original units. The Gibbs-free energy to two loops (finite parts of the integrals were calculated numerically) is

$$G = \frac{eBk_BT}{L_z\pi\hbar c}g,$$

$$g = -\frac{1}{2\beta_A}a_T^2 + \frac{1}{2\pi}\ln(|a_T|) + c\frac{1}{a_T^2}, \qquad (34)$$

where numerical values of the coefficient is $c = -5.2$. The dimensionless entropy (the LLL scaled magnetization) is
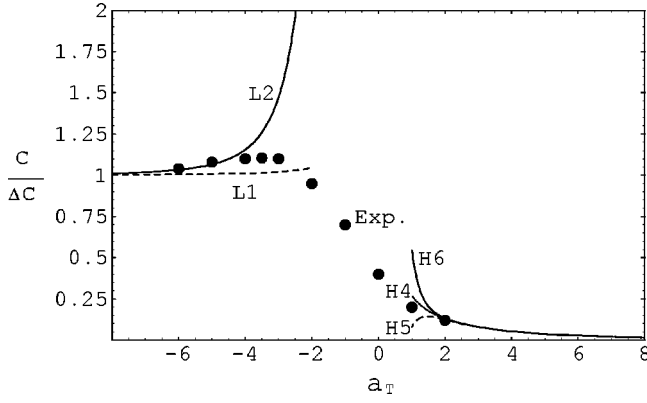
FIG. 3. Comparison between low-temperature and high-temperature expansion of the scaled specific heat defined in Eq. (36).

$$s = -\frac{dg}{da_T} = \left(\frac{L_z \pi c^3 m_{ab}^2 b'}{\hbar e^5 k_B}\right)^{1/3} \frac{M}{(TB)^{1/2}}$$

$$= \frac{1}{\beta_A} a_T - \frac{1}{2\pi}\frac{1}{a_T} + 2c\frac{1}{a_T^3}, \tag{35}$$

and the specific heat normalized to the mean-field value is

$$\frac{1}{\beta_A}\frac{C}{\Delta C} = -\frac{d^2 g}{da_T^2} = \frac{1}{\beta_A} + \frac{1}{2\pi}\frac{1}{a_T^2} - 6c\frac{1}{a_T^4}. \tag{36}$$

We first compare the results with those of the high-temperature expansion.[3] These series are known now to the 12th order in x.[15] Successive partial sums for specific heat at low temperature are plotted on Fig. 3 (dashed lines) together with several orders of the high-temperature expansion. Low-temperature expansion indicates that the specific heat ratio grows with a_T. On the other hand, the high-temperature expansion clearly shows that it drops out quickly above $a_T = 0$. This means that there is a maximum in between that is consistent with most experiments and Monte Carlo simulations, see Fig. 4. Whether there is a melting phase transition either first order or continuous (in 2D it is necessarily of the Kosterlitz-Thouless variety) cannot be determined from series alone. Both series expansions have a finite radius of convergence, but this fact alone is not enough to decide that
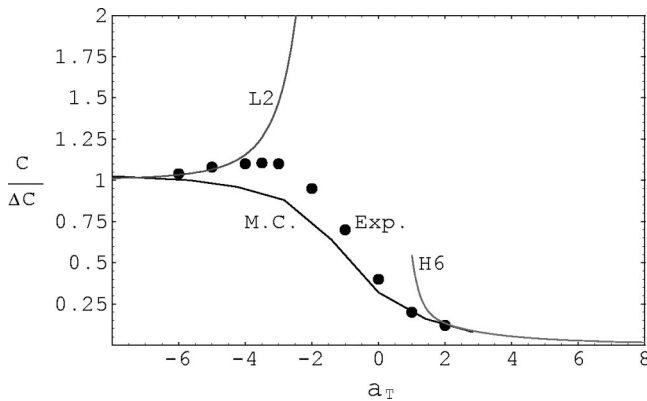

FIG. 4. Comparison between theoretical, experimental, and Monte Carlo results of the scaled specific heat.

the singularity is at real temperature (it can be located in the complex plane as, for example, in the one-dimensional Ising model). The low-temperature series are too short to estimate the radius of convergence. Naively comparing the second coefficient in specific heat [Eq. (36)] to the third one obtains an estimate $a_T = -\sqrt{12\pi c_3} = -8$. Phenomenologically first-order melting occurs around $a_T = -10$. Extensive analysis of the high-temperature series has been made in Refs. 15 and 16.

B. Comparison with MC, experiments, and other theoretical results

Low-temperature results for free energy and magnetization agree well with available numerical simulations and experiments. However specific heat comparison is the most sensitive (second derivative). We, therefore, present here only the specific heat comparison. For $a_T < -5$ the specific heat results on Fig. 4 are in accord qualitatively with experiments of Ref. 17, and MC simulations of Ref. 10. The same data were fitted by the theory of Tesanovic and co-workers.[11] We can calculate the coefficients of the low-energy expansions from their theory and we get

$$\frac{1}{\beta_A}\frac{C}{\Delta C} = \frac{1}{\beta_A} - 2\frac{1}{a_T^2} + 12\beta_A\frac{1}{a_T^4}$$

compared to our Eq. (36). Even the sign of the $1/a_T^2$ contribution is different. This theory is only an approximate one and perhaps some modifications are required in the low-temperature limit.

V. UNDERSTANDING CANCELLATIONS OF INFRARED DIVERGENCIES IN A SIMPLE MODEL. NONPERTURBATIVE EFFECTS

A. Toy model

The dramatic cancellation of all the severe IR divergencies in the GL LLL model up to L^8 at the two-loop level looks a bit mysterious. Although in critical phenomena the phenomenon of cancellation of ''spurious'' divergencies due to Goldstone bosons is well known,[18] here it occurs under rather extreme circumstances. The theory is below its lower critical dimensionality. To better understand what is involved in these cancellations we investigated a model that has similar symmetry properties, but is much simpler. As was mentioned in the introduction the physics of the D-dimensional GL theory is very reminiscent of that of the (D-1)-dimensional scalar theory with two fields possessing a continuous $O(2)$ symmetry, see Fig. 5,

$$F = \frac{1}{2}(\dot{\varphi}_a)^2 + a_T\varphi_a^2 + \frac{1}{2}(\varphi_a^2)^2,$$

where the overdot denotes the derivative in the only dimension considered as ''time'' and we are interested in the spontaneously broken symmetry case $a_T < 0$.

This model is equivalent to quantum mechanics of the two dimensional anharmonic oscillator. Of course one can solve this model nonperturbatively (albeit using numerical solution of the differential equation, we are not aware of the closed form of the ground-state energy). Obviously the result
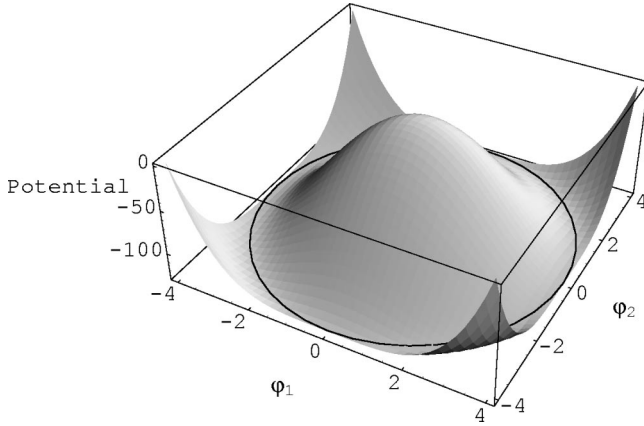
FIG. 5. Potential of the anharmonic oscillator. The classical ground state indicated by the circle is degenerate.

is IR finite (bounded from below by the classical energy and from above by variational Gaussian energy).[19]

B. Perturbation theory

It is important to trace the origin of the IR divergencies in the intermediate steps of the perturbative calculation. Although the calculation has been done using Feynman diagrams (steepest descent approximation of the path integral), like in the GL model above, it is useful to start from the standard time-independent perturbation theory. Here we first have to decide what is the main part K and what will be a perturbation V. The perturbative vacuum in which $\langle \varphi_a \rangle = v_a$ is degenerate and we have many choices of the "unperturbed" part. One of them corresponding to the choice

$$v_a = (\sqrt{-a_T}, 0) \equiv (v, 0),$$

$$O \equiv \varphi_1 - v, \quad A \equiv \varphi_2$$

is

$$H = -\frac{a_T^2}{2} + K + V,$$

$$K = \frac{1}{2}(\pi_O^2 + \pi_A^2) + 2v^2 O^2 + \frac{1}{2L^2} A^2,$$

$$V = 2v(O^3 + OA^2) + \frac{1}{2}(O^2 + A^2)^2,$$

where π_O and π_A are conjugate momenta of the fields O and A, respectively. The constant in H is the classical energy. Since any of these ground states are non-normalizable, see Fig. 5, the IR cutoff L was introduced into K. It also removes the vacuum degeneracy. With this cutoff the unperturbed wave function is

$$\Psi_{0,0}(\varphi_1, \varphi_2) = \left(\frac{2v}{\pi^2 L}\right)^{1/4} \exp\left[-\frac{1}{2L}\varphi_2^2 - v(\varphi_1 - v)^2\right].$$

Zero-point energy $\langle \Psi_{0,0} | V | \Psi_{0,0} \rangle$ corresponds in the time-dependent perturbation theory to

$$F_1 = \frac{1}{2}(\operatorname{Tr}\ln G_O + \operatorname{Tr}\ln G_A) = v + O\left(\frac{1}{L}\right)$$

in the time-dependent formalism. The leading correction to the ground-state energy is

$$F_2^{bb} = \langle \Psi_{0,0} | V | \Psi_{0,0} \rangle = \frac{3L^2}{8} + \frac{L}{8}\frac{1}{v} + \frac{3}{32}\frac{1}{v^2} + O\left(\frac{1}{L}\right).$$

It is equal to three "double-bubble diagrams of Fig. 2. The second order in the V correction is

$$F_2^{ss} = \sum_{(n1,n2)\neq(0,0)} \frac{|\langle \Psi_{0,0} | V | \Psi_{n1,n2}\rangle|^2}{E_{0,0} - E_{n1,n2}}$$

$$= \frac{|\langle \Psi_{0,0} | V | \Psi_{1,0}\rangle|^2}{-2v} + \frac{|\langle \Psi_{0,0} | V | \Psi_{3,0}\rangle|^2}{-6v} + \frac{|\langle \Psi_{0,0} | V | \Psi_{1,2}\rangle|^2}{-2v - \frac{2}{L}}$$

$$= -\frac{3L^2}{8} - \frac{L}{8}\frac{1}{v} - \frac{19}{32}\frac{1}{v^2} + O\left(\frac{1}{L}\right).$$

This contribution is the sum of the "setting-sun diagrams" and correction terms (some terms that contain higher orders in $1/a_T$ were dropped). Unlike the GL theory there is no AAA setting-sun diagram and therefore no L^4 divergence is expected. The leading divergence L^2 and the subleading L cancel between F_2^{bb} and F_2^{ss}.

C. Absence of long-range order

As is well known even discrete symmetry cannot be broken spontaneously in 1D. This means that when we calculate the perturbatively vacuum expectation value (VEV) of a quantity that is not invariant under the symmetry group $O(2)$, it should be IR divergent.[14] As an example we calculate the expectation value of φ_1. The first-order correction to $\langle \Psi | \varphi_1 | \Psi \rangle$ arises from the corrected ground state

$$\Psi = \Psi_{0,0} + \sum_{(n1,n2)\neq(0,0)} c_{n1,n2} \Psi_{n1,n2},$$

$$c_{n1,n2} = \frac{\langle \Psi_{0,0} | V | \Psi_{n1,n2}\rangle}{E_{0,0} - E_{n1,n2}},$$

$$c_{1,0} = -\frac{2vL + 3}{8v^{3/2}}.$$

The result is

$$\langle \Psi | \varphi_1 | \Psi \rangle = v + 2c_{1,0}\langle \Psi_{0,0} | O | \Psi_{1,0}\rangle = \sqrt{-a_T} - \frac{1}{\sqrt{-a_T}}\frac{L}{4}.$$

It diverges linearly indicating "dynamical restoration" of the symmetry. The sign of the correction indicates that the VEV is reduced. The exact finite size expression is nonanalytic (like $\sqrt{-a_T}\exp[L/4\sqrt{-a_T}]$) and approaches zero.

This model clearly teaches us that although the $O(2)$ symmetry is unbroken, the perturbation theory starting from the "broken" symmetry ground state not only cures its own IR divergency problems, but provides an accurate approxi-

mation to any $O(2)$ symmetric quantity. Perturbation theory actually ''knows'' about restoration of the symmetry missing only corrections of the essential singularity variety.

VI. CONCLUSION

To summarize, it is established up to order of two loops that the perturbation theory around the Abrikosov lattice is consistent. All the IR divergencies cancel due to soft interactions of the soft mode. Perturbative results as well as interpolation with the high-temperature expansion agree very well with the direct MC simulation and experiments. In the theory of Tešanović et al.,[11] all the thermodynamic quantities are expressed in terms of the variable g and the function $U(g)$. More specifically, $g = a_T/\sqrt{2}$, and $U(g)$ is chosen to be

$$U(g) = \frac{1}{2}\left(\frac{1}{\sqrt{\beta_A}} + \frac{1}{\sqrt{2}}\right) - \frac{1}{2}\left(\frac{1}{\sqrt{\beta_A}} - \frac{1}{\sqrt{2}}\right)\tanh\left[\frac{g+\sqrt{2}}{2\sqrt{2}}\right],$$

so that it is monotonic and approaches the desired asymptotic values in the low- and high-temperature limits. To compare their result in Eq. (7) with ours, let us note that the scaled magnetization defined there differs from ours by a factor $\sqrt{2}$. Their results have a different low-temperature limit from ours and can be modified easily. For example, we can add an rational function such as $(a_0 + a_2 g^2)/(b_0 + g^4)$ to $U(g)$. By choosing $a_0 = 1.5$ and $a_2 = -0.23$, we can make the two low-temperature expansions consistent. Since b_0 has no effect in the expansion to this order, we can choose it as large as we want (e.g., 1000) so that the function $U(g)$ remains monotonic.

Consistency of the perturbation theory rules out a possibility of an infinite lattice at any $T > 0$. Let us briefly summarize what it physically means and under what conditions this result is valid. The fact that v is IR divergent in both 2D (power) and 3D (logarithm) means that order parameter of translational symmetry breaking vanishes. Its correlator at very large distances approaches zero. This does not necessarily mean that the state is liquid, namely, the correlator decays exponentially with certain correlation length. It might decay only as a power like in the two-dimensional XY model[20] and melt into liquid via either first-order or continuous transition. The assumptions are no disorder, infinite sample, LLL approximations, and no fluctuations of the magnetic field. The third assumption can be relaxed since one obtains a supersoft $1/k^4$ spectrum also after including higher Landau levels, see Refs. 12 and 13; however, including fluctuations of the magnetic field will probably stabilize the lattice in 3D since the spectrum becomes the usual Goldstone boson $1/k^2$.

APPENDIX: SMALL MOMENTUM EXPANSION OF FEYNMAN DIAGRAMS

In this appendix we give formulas for expansion of integrands in powers of quasimomenta, which is needed to eighth order. The basic quantity that enter the Feynman diagrams is the function λ. Using identities between the coefficients β defined in Eq. (33), $\beta_{02} = \frac{1}{2}\beta_{00}$, $\beta_{04} = \frac{3}{2}\beta_{00} - 3\beta_{22}$, we have

$$\lambda(\mathbf{k}_1, \mathbf{k}_2) = \exp\left\{-\frac{(k_1^x)^2 + (k_2^x)^2}{2}\right\}\beta_{00} + \frac{1}{4}\beta_{00}[(k_2^x - ik_1^y)^2$$

$$+ (k_1^x - ik_2^y)^2] + \frac{1}{16}\beta_{00}[(k_2^x - ik_1^y)^4 + (k_1^x - ik_2^y)^4]$$

$$- \frac{1}{8}\beta_{22}[-(k_2^x - ik_1^y)^2 + (k_1^x - ik_2^y)^2]^2$$

$$+ \frac{1}{720}\beta_{06}[(k_2^x - ik_1^y)^6 + (k_1^x - ik_2^y)^6] + \frac{1}{48}\beta_{24}(k_2^x$$

$$- ik_1^y)^2(k_1^x - ik_2^y)^2[(k_2^x - ik_1^y)^2 + (k_1^x - ik_2^y)^2]$$

$$+ \frac{1}{40320}\beta_{08}[(k_2^x - ik_1^y)^8 + (k_1^x - ik_2^y)^8]$$

$$+ \frac{1}{1440}\beta_{26}(k_2^x - ik_1^y)^2(k_1^x - ik_2^y)^2[(k_2^x - ik_1^y)^4$$

$$+ (k_1^x - ik_2^y)^4] + \frac{1}{576}\beta_{44}(k_2^x - ik_1^y)^4(k_1^x - ik_2^y)^4.$$

[1] E. Brezin, D. R. Nelson, and A. Thiaville, Phys. Rev. B **31**, 7124 (1985).

[2] M. Tinkham, *Introduction to Superconductivity* (McGraw-Hill, New York, 1996).

[3] D. J. Thouless, Phys. Rev. Lett. **34**, 946 (1975); G. I. Ruggeri and D. J. Thouless, J. Phys. F: Met. Phys. **6**, 2063 (1976); S. Hikami, A. Fujita, and A. I. Larkin, Phys. Rev. B **44**, 10 400 (1991). See also Ref. 15.

[4] B. Rosenstein, Phys. Rev. B **60**, 4268 (1999).

[5] G. J. Ruggeri, J. Phys. F: Met. Phys. **9**, 1861 (1979); M. A. Moore, Phys. Rev. B **45**, 7336 (1992).

[6] G. Eilenberger, Phys. Rev. **164**, 628 (1967).

[7] K. Maki and H. Takayama, Prog. Theor. Phys. **46**, 1651 (1971).

[8] G. J. Ruggeri, Phys. Rev. B **20**, 3626 (1979).

[9] F. David, Commun. Math. Phys. **81**, 149 (1981).

[10] Y. Kato and N. Nagaosa, Phys. Rev. B **48**, 3464 (1993).

[11] Z. Tešanović et al., Phys. Rev. Lett. **69**, 3563 (1992); Z. Tešanović and A. V. Andreev, Phys. Rev. B **49**, 4064 (1994); S. W. Pierson et al., *ibid.* **57**, 8622 (1998).

[12] H. Ikeda, T. Ohmi, and T. Tsuneto, J. Phys. Soc. Jpn. **58**, 1377 (1989).

[13] D. Li and B. Rosenstein, cond-mat/9902294 (unpublished).

[14] A. Jevicki, Phys. Lett. **71B**, 327 (1977).

[15] S. Hikami, A. Fujita, and A. Larkin, Phys. Rev. B **44**, 10 400

(1991).

[16] N. K. Wilkin and M. A. Moore, Phys. Rev. B **47**, 957 (1993).

[17] J. S. Urbach, W. R. White, M. R. Beasley, and A. Kapitulnik, Phys. Rev. Lett. **69**, 2407 (1992).

[18] I. D. Lawrie, Phys. Rev. B **50**, 9456 (1994).

[19] P. M. Stevenson, Phys. Rev. D **23**, 2916 (1981); A. Kovner and B. Rosenstein, *ibid.* **39**, 2332 (1989); **40**, 504 (1989).

[20] V. L. Berezinskii, Zh. Éksp. Teor. Fiz. **59**, 907 (1970) [JETP **32**, 493 (1971)]; J. V. Jose, L. P. Kadanoff, S. Kirkpatrick, and D. Nelson, Phys. Rev. B **16**, 1217 (1977).